HHS Public Access

Author manuscript

Clin Cancer Res. Author manuscript; available in PMC 2019 June 01.

Published in final edited form as:

Clin Cancer Res. 2018 June 01; 24(11): 2616–2630. doi:10.1158/1078-0432.CCR-17-1207.

The transcriptional co-activator TAZ is a potent mediator of alveolar rhabdomyosarcoma tumorigenesis

Michael D. Deel[1], **Katherine K. Slemmons**[2], **Ashley R. Hinson**[1], **Katia C. Genadry**[1], **Breanne A. Burgess**[1], **Lisa E.S. Crose**[1], **Nina Kuprasertkul**[3], **Kristianne M. Oristian**[1], **Rex C. Bentley**[4], and **Corinne M. Linardic**[1,2]

[1]Division of Hematology-Oncology, Department of Pediatrics, School of Medicine, Duke University, Durham, NC USA

[2]Department of Pharmacology & Cancer Biology, School of Medicine, Duke University, Durham, NC USA

[3]Duke University, Durham, NC USA

[4]Department of Pathology, School of Medicine, Duke University, Durham, NC USA

Abstract

Purpose: Alveolar rhabdomyosarcoma (aRMS) is a childhood soft tissue sarcoma driven by the signature *PAX3-FOXO1* (P3F) fusion gene. 5-year survival for aRMS is <50%, with no improvement in over four decades. Although the transcriptional co-activator TAZ is oncogenic in carcinomas, the role of TAZ in sarcomas is poorly understood. The aim of this study was to investigate the role of TAZ in P3F-aRMS tumorigenesis.

Experimental Design: After determining from public datasets that TAZ is upregulated in human aRMS transcriptomes, we evaluated whether TAZ is also upregulated in our myoblast-based model of P3F-initiated tumorigenesis, and performed IHC staining of 63 human aRMS samples from tissue microarrays. Using constitutive and inducible RNAi, we examined the impact of TAZ loss-of-function on aRMS oncogenic phenotypes *in vitro* and tumorigenesis *in vivo*. Last, we performed pharmacological studies in aRMS cell lines using porphyrin compounds, which interfere with TAZ-TEAD transcriptional activity.

Results: TAZ is upregulated in our P3F-initiated aRMS model, and aRMS cells and tumors have high nuclear TAZ expression. *In vitro*, TAZ suppression inhibits aRMS cell proliferation, induces apoptosis, supports myogenic differentiation, and reduces aRMS cell stemness. TAZ-deficient aRMS cells are enriched in G2/M. *In vivo*, TAZ suppression attenuates aRMS xenograft tumor growth. Preclinical studies show decreased aRMS xenograft tumor growth with porphyrin compounds alone and in combination with vincristine.

Conclusions: TAZ is oncogenic in aRMS sarcomagenesis. While P3F is currently not therapeutically tractable, targeting TAZ could be a promising novel approach in aRMS.

Corresponding author Corinne M. Linardic; Box 102382 DUMC, Durham, NC, 27710; linar001@mc.duke.edu.
Reprint requests
Corinne M. Linardic, Box 102382 DUMC, Durham, NC, 27710; linar001@mc.duke.edu.

Conflicts of interest The authors declare no potential conflicts of interest.

Keywords

TAZ; WWTR1; rhabdomyosarcoma; Hippo; PAX3-FOXO1

Introduction

Rhabdomyosarcoma (RMS) is the most common soft tissue sarcoma of childhood. Originating from primitive mesenchymal tissue and associated with the skeletal muscle lineage (1,2), RMS is comprised of two histologic subtypes: embryonal (eRMS), which accounts for the majority of cases, and alveolar (aRMS), which accounts for 20% of cases. Both eRMS and aRMS are treated with multi-modal therapy consisting of chemotherapy, surgery, and/or radiation. Standardization of management through collaborative clinical trials improved RMS survival rates from 25% in the 1970s to 70% in the 1990s. Vincristine, dactinomycin, and cyclophosphamide (VAC), a combination first identified in the 1970s, became the accepted chemotherapy regimen. However, subsequent clinical trials have failed to identify other regimens or targeted agents superior to VAC (3). While the 5-year overall survival rates for eRMS and fusion negative (PF-neg) aRMS are approaching 80% (4), survival for patients with fusion-positive aRMS remains stagnant at less than 50%. Most aRMS tumors are characterized by signature t{2;13} or t{1;13} chromosomal translocations that encode the PAX3-FOXO1 (P3F) and PAX7-FOXO1 (P7F) fusion proteins, respectively. These oncogenic chimeric transcription factors are usually the sole DNA mutation in an otherwise quiet genome, and thought to be the main drivers of aRMS tumorigenesis (5,6). Metastasis, chemoresistance, and/or relapse are common (4,7), underscoring the need for novel effective therapies.

Our previous investigations into proteins that collaborate with P3F in aRMS tumorigenesis revealed a role for Hippo/MST1 kinase inactivation (8). The Hippo pathway plays a vital role in tissue growth and homeostasis, organ size control, and tumor suppression (9,10). The core of the Hippo pathway is an MST1/2-LATS1/2 kinase cascade, which phosphorylates and inactivates two downstream effectors known as YAP (Yes-associated protein) and its less studied paralog TAZ (transcriptional co-activator with PDZ-binding motif). YAP and TAZ are encoded by the *YAP1* and *WWTR1* (WW domain containing transcriptional regulator 1) genes, respectively. Phosphorylation of YAP and TAZ, which occurs at five (YAP) and four (TAZ) serine residues, respectively, leads to YAP/TAZ cytoplasmic retention through the binding of 14–3-3 proteins at phospho-S127 (YAP) or phospho-S89 (TAZ), as well as β-TRCP-dependent proteasomal degradation (11). When unphosphorylated, YAP and TAZ localize to the nucleus and co-activate pro-growth transcription factors (12,13), most notably the TEAD family (14,15). Functionally, YAP/TAZ are essential for cellular proliferation, amplification of tissue-specific progenitor cells during tissue regeneration, and ultimately control of organ size (11,16). In many contexts, YAP and TAZ have overlapping roles. However, they share only 50% homology and have divergent functions in development. For example, YAP knockout mice are embryonic lethal, while TAZ knockout mice are viable but frequently develop polycystic kidney disease (17,18). In skeletal muscle homeostasis YAP inhibits myogenesis (19), while TAZ enhances myogenic differentiation by associating with and activating MyoD-induced gene expression (20).

The roles of YAP/TAZ in epithelial malignancy have been widely studied. For example, in breast cancer TAZ binds to TEADs to potentiate invasion and metastasis (21,22) as well as cancer stem-like properties and chemoresistance (23). Similarly, in hepatocellular carcinoma and malignant glioma, TAZ promotes tumorigenesis, supports stemness, and mediates epithelial to mesenchymal transition (24,25). However, an understanding of the roles of YAP and TAZ in mesenchymal cancers, including RMS, is just beginning. In eRMS, higher YAP/TAZ expression at the IHC level correlates with reduced patient survival (8,26,27), and a subset of tumors have copy number gains in the *YAP1* and/or *WWTR1* loci (26,27). YAP contributes to eRMS tumorigenesis by supporting proliferation and stemness, and opposing myogenic differentiation (8,26,28), potentially at the early steps of tumorigenesis based on a human myoblast model of eRMS (28). Similarly, TAZ contributes to eRMS by supporting proliferation, colony formation, and increasing the expression of select cancer-related genes (27). Expression of TAZS89A (a constitutively active TAZ mutant) transforms C2C12 myoblasts (27), again suggesting that YAP/TAZ exert oncogenic effects early during tumorigenesis.

Less is known about the roles of YAP/TAZ in aRMS. We had previously shown that YAP is highly abundant in P3F-aRMS cells, supporting proliferation and evasion of senescence (8). Given this, we expected to find in our previously established myoblast-based model of P3F-initiated tumorigenesis that *YAP1* would be upregulated. Instead, *WWTR1* was increased at the mRNA level in this model, suggesting that TAZ has a specific role in aRMS tumorigenesis. A potential functional role for TAZ in aRMS is further suggested by studies showing that TAZ is essential to the transcriptional activity of wild type PAX3 (29,30) and that the binding of TAZ to PAX3 occurs via domains that are retained in the P3F fusion (5). The aim of this study was to elucidate the oncogenic activity of TAZ in P3F-aRMS sarcomagenesis.

Materials and Methods

Generation of Cell Lines and Constructs

Human RMS cell lines Rh28 (31) and Rh30 (32) were gifts from Tim Triche (Children's Hospital of Los Angeles, CA, USA) in 2005; Rh3 (33), Rh41 (34), and CW9019 (35) were gifts from Brett Hall (Columbus Children's Hospital, OH, USA) in 2006. All cell lines tested negative for Mycoplasma (using Lonza MycoAlert PLUS test at the Duke University cell culture facility) and were also authenticated by STR analysis (Promega Powerplex 18D at Duke University DNA analysis facility) in 2014; Rh28 and Rh30 were re-authenticated in 2016. Human skeletal muscle myoblasts (HSMMs) and 293T cells were obtained from Lonza (Walkersville, MD) and the ATCC through the Duke University Cell Culture Facility, respectively, and cultured as described (36). Knockdown and overexpression constructs described below were stably expressed using established lentiviral and selection methods resulting in polyclonal cell lines (37). TAZ shRNA oligos (23,38) or non-targeting (NT) scrambled controls (Supplementary Table I) were annealed and ligated into pLKO.1-puro or Tet-pLKO-puro (Addgene plasmids #8435 and #21915, respectively). Lenti-EF-ires-blast and pLenti-EF-FH-TAZ S89A-ires-blast (Addgene #52084) vectors were gifts from Yutaka Hata (Tokyo Medical and Dental University, Tokyo, Japan). pQCXIH-Flag-YAP-S127A

(Addgene 33092) was a gift from Kun-Liang Guan (University of California San Diego, CA, USA) (39).

Growth Curves, MTT, BrdU, and Cell-Cycle Analysis Assays

Standard growth curves using manual and automated hemocytometer counting, as well as MTT and BrdU assays, were performed as described (40). Cell-cycle analyses were performed and analyzed by the Duke University Flow Cytometry core as described (41).

Differentiation Assays

Differentiation assays and MF20 (DSHB Hybridoma Product MF20) staining were performed as described (37) except that on day 0, Rh28 and Rh30 cells were plated at a density of 5×10^5 and 2.5×10^5/6cm dish, respectively. Positively and negatively staining cells (five images per condition), were counted manually with the aid of cell counting software (ImageJ, NIH).

Rhabdosphere and Limiting Dilution Assays

To establish and propagate aRMS cell spheres, we modified a protocol developed for eRMS cells (42). Briefly, aRMS cells were grown in ultra-low attachment plates or flasks (Corning) in Neurobasal media (Gibco) supplemented with 1X B27 [2X B27 for Rh28 cells] (Invitrogen), 80ng/ml bFGF (Corning), 40ng/ml EGF (Sigma), and 50μg/ml insulin. Limiting dilution assays were based on sphere formation, and assessed 48 wells per condition. Wells were scored positive (≥ 1 sphere/well) or negative (0 spheres/well) for sphere formation after seven days in culture. Sphere forming frequency and statistics were calculated using ELDA software (43).

Luciferase Reporter Assays

Rh28 (100,000 cells/well) or Rh30 (50,000 cells/well) cells stably expressing TAZ shRNA, TAZS89A, or NT vector were transiently transfected with TEAD luciferase reporter (8X GTIIC plasmid) or empty vector (pGL3-E-P) and 5ng of Renilla reporter (pHRC TR1) for 48 hours in triplicate in 24-well plates. Treatment (see Drug Treatment section below) with verteporfin (VP) or protoporphyrin IX (PPIX) was performed for 24h prior to reading. Luciferase activity was assayed using the Dual Luciferase Reporter Assay (Promega) per manufacturer's protocol in a luminometer (Turner Biosystems Modulus). Data are presented as Firefly/Renilla luciferase activity.

Cell-fractionation, qRT-PCR, and Immunoblotting

For cell-fractionation, 1×10^6 cells were plated in a 10cm dish; after 48h in culture they were trypsinized, washed, and fractionated into subcellular components using a detergent-based kit (Cell Signaling #9038). Quantitative real-time PCR (qRT-PCR) was performed as described (8) using primer sets listed in Supplementary Table I. Immunoblotting was performed as described (40) using anti-TAZ, anti-PARP, anti-cleaved PARP (Asp214), anti-phospho-histone (Cell Signaling #4883, #9542, #9541, #9701), anti-β-tubulin, anti-actin (Sigma #T8328, #A5441), anti-histone H3 (Abcam ab1791) and anti-MF20 (DSHB Hybridoma Product MF20) antibodies.

Mouse Xenograft Studies

Xenograft studies utilized 10×10^6 Rh28 cells resuspended in Matrigel (BD Biosciences) and implanted subcutaneously (SQ) into the flanks of immunodeficient SCID/*beige* mice as done previously (8,44). For the TAZ shRNA study, Rh28 cells stably expressing doxycycline-inducible TAZ shRNAs were used. The drinking water was supplemented with 1mg/ml doxycycline (Sigma-Aldrich) in 5%w/v sucrose or 5%w/v sucrose (control). Mice were monitored twice weekly, and upon observing palpable tumors, randomly assigned to the doxycycline or sucrose group. We had previously demonstrated no difference in tumor growth dynamics in Rh28 cell xenografts with a NT vector control in mice treated with doxycycline versus sucrose (8,44). Tumors were measured using calipers and tumor volume calculated as $[((\text{width}*\text{length})/2)^3]/2$. Mice were sacrificed upon reaching an IACUC-defined maximum tumor burden ($2000m^3$) or decline in health (TAZ shRNA study), or after 28 days from development of a palpable tumor (VP studies). Portions of tumors were preserved in RNAlater (Qiagen) for PCR or formalin-fixed and paraffin-embedded (FFPE) for IHC.

Immunohistochemistry

Human RMS tissue microarrays (TMAs) were obtained through the Children's Oncology Group (COG) from the Biopathology Center at Nationwide Children's Hospital (Columbus, Ohio, USA), and contained cores of 63 (in the TAZ analysis) or 64 (in the YAP analysis) unique aRMS tumors from 217 tissue samples that were suitable for analyzing. TAZ analysis included 34 P3F, 13 P7F, and 13 PF-neg aRMS tumors. YAP analysis included 36 P3F, 10 P7F, and 15 PF-neg aRMS tumors (See Supplementary Table 2). Three aRMS tumors from each TMA were not annotated for fusion status; these were included in the overall analysis (Supplementary Fig. 3F) but were excluded from the fusion status subset analyses. TAZ and YAP immunostaining were performed as previously described (8,28) using TAZ (Sigma #HPA007415) and YAP (Cell Signaling #4912) antibodies per the manufacturer's protocols. Specifically, we performed antigen retrieval by heating slides for 4min at 125°C in a pressure cooker, followed by incubation with primary antibody at a 1:50 dilution overnight at 4°C. Expression was scored by two blinded observers using a semi-quantitative method (8) based on the relative amount of nuclear staining. Scoring standards are shown in Supplementary Fig. 1. Of note, we had previously reported YAP staining of eRMS and aRMS cases (8) prior to aRMS subtype annotation from the COG. Therefore, the YAP TMA was re-analyzed taking into consideration the annotation and re-classification, which resulted in two eRMS tumors being re-classified as aRMS, and two aRMS tumors being re-classified as eRMS. Details of the TMA cases are in Supplementary Table 2.

In separate studies, FFPE xenograft tumors samples were similarly immunostained and scored for YAP and TAZ expression (standards in Supplementary Fig. 2), and also H&E (Sigma #HHS16, HT110316), Ki67 (Dako #M7240) and TUNEL (Trevigen #4810–30-K) per the manufacturer's protocols (8,28). Slides were photographed, positively and negatively stained cells were counted manually with the aid of cell counting software (ImageJ, NIH), and 4–5 images counted per condition. Tumor samples were examined by a pathologist (R.C.B.) with experience in pediatric sarcomas.

Drug Treatments

For *in vitro* studies, VP (Proactive Molecular Research P17–0440), PPIX (Sigma P8293), and vincristine sulfate (VCR) (Hospira) were dissolved in DMSO: PPIX and VP at 100mg/ml stock, and VCR at 10μM stock. In cell culture media, VP and PPIX were further diluted to 10μM, and VCR to 100nM. For *in vivo* experiments, two studies were evaluated: (i) DMSO vs. VP and (ii) DMSO vs. VP vs. VCR vs. VCR plus VP. Drugs were diluted in PBS to a concentration of 10% DMSO, 10mg/ml VP, or 1mg/ml VCR and administered by intraperitoneal (IP) injection. Upon palpable tumors, mice were randomly assigned to treatment groups of equal number and were dosed with DMSO, 100mg/kg VP, and/or 1mg/kg VCR. DMSO and VP were administered every other day for eight total treatments. VCR was administered weekly for four total treatments. Tumors were harvested at day 28 following tumor formation. A 28-day duration of therapy was pre-determined in the study design as prior xenografts studies using 10×10^6 Rh28 cells had reached maximum tumor burden by this point (8,44).

Microarray

Microarray analysis of transcriptional changes in HSMMs stably expressing P3F was previously described (8,36). The associated dataset was deposited in the Gene Expression Omnibus database (accession GSE40543).

Study Approval

All animal studies were performed under Duke University Institutional Animal Care and Use Committee (IACUC)-approved protocols. Human TMAs obtained from the COG had been generated from de-identified patient tissue collected with informed consent and were approved for use by the Institutional Review Board of Duke University.

Statistical Analysis

Unless noted, experiments were performed in at least three experimental replicates, and data is presented as the mean and standard error. Statistical analysis was performed using GraphPad Prism (GraphPad). One-way ANOVA, two-way ANOVA, Log-Rank (Mantel-Cox) Test, unpaired T-test, and Pearson's correlation coefficient were used as appropriate. P values were considered significant under 0.05, with *, $P<0.05$; **, $P<0.01$; and ***, $P<0.001$

Results

WWTR1/TAZ is upregulated in PAX3-FOXO1 (P3F)-expressing primary human skeletal muscle myoblasts, aRMS cell lines, and aRMS tumors

To gain insight into genes regulated by P3F, our laboratory developed a cell-based model of aRMS based on P3F-initiated transformation of HSMMs. In brief, forced expression of P3F in combination with $p16^{INK4A}$ loss in HSMMs enabled senescence bypass (37); additional expression of hTERT and MycN yielded cells that formed tumor xenografts histologically mimicking human aRMS (45). Microarray analysis of P3F-initiated transformation of HSMMs revealed upregulated expression of *RASSF4,* which is a transcriptional target of P3F and promotes aRMS tumorigenesis by restraining the Hippo tumor suppressor kinase

MST1 (8). Since the transcriptional co-activator YAP is a critical downstream effector of oncogenic Hippo signaling, we anticipated finding that *YAP1* would also be upregulated. However, analysis of the microarray dataset showed that *YAP1* expression was unchanged, while *WWTR1* (encoding TAZ) was upregulated (Fig. 1A). These findings were validated by qRT-PCR using cDNA generated from the original cells represented in the microarray (Fig. 1B,C). While the increase in expression was only about two-fold, other genes known to be targets of P3F, such as *IL4R (46,47)*, were also only upregulated about two-fold (Fig. 1D), suggesting that the increase in TAZ could be important.

After confirming that TAZ was upregulated in the HSMM-based model, we examined *WWTR1* mRNA and TAZ protein expression in a panel of P3F or P7F fusion-positive human aRMS cell lines. In contrast to quiescent mature skeletal muscle, both *WWTR1* and TAZ expression were significantly higher in aRMS (Fig. 1E,F). To determine whether this occurred in human aRMS tumors, we queried the NIH Pediatric Oncology Branch Oncogenomics database (48) and found that *WWTR1* mRNA levels are higher in human aRMS tumors than in skeletal muscle (Fig. 1G). Using the same human RMS TMA block that we had previously used to analyze YAP (8), we examined TAZ protein expression by IHC. Compared to skeletal muscle, where TAZ is membrane-bound or cytoplasmic, in aRMS tumors TAZ was predominantly nuclear (Fig. 1H). This held true for P3F, P7F, and PF-neg tumors. Interestingly, TAZ abundance is not specific to P3F aRMS and was also observed in P7F aRMS, PF-neg aRMS, and eRMS cases (Fig. 1I, Supplementary Fig. 3A-C), suggesting that TAZ is important for RMS tumorigenesis across the mutational landscape. Because TAZ was upregulated in our P3F-initiated model, and because TAZ is a critical co-activator for wild-type *PAX3* in other cell types (29,30), we focused our studies on P3F-positive aRMS.

Since TAZ and YAP have overlapping functions and YAP is also abundant in aRMS (8), we hypothesized that individual tumors might preferentially express one or the other, as seen in malignant peripheral nerve sheath tumors (49). To determine whether TAZ and YAP abundance inversely correlated, we re-analyzed the TMA previously immunostained for YAP (8) and observed a similar degree of YAP expression among the P3F, P7F, and PF-neg aRMS groups (Fig. 1J,K, Supplementary Fig. 3D). In the nine P3F-aRMS tumors where YAP was scored as 1 (<25% nuclear staining), two had a TAZ score of 2 and seven had a TAZ score of 3. However, using a Pearson's correlation coefficient, TAZ and YAP levels do not significantly correlate in P3F-aRMS samples, in the other subgroups, or overall in aRMS (Supplementary Fig. 3E,F). This suggests that most aRMS tumors co-express TAZ and YAP, which was also observed in synovial sarcoma (49).

TAZ suppression inhibits P3F-aRMS cell growth

After determining TAZ abundance in human aRMS cell lines and tumor tissue, we sought to determine the phenotypic consequence of TAZ loss-of-function in Rh28 and Rh30 (both P3F-positive) human aRMS cell lines. However, because prior reports had noted mostly cytoplasmic TAZ in aRMS IHC studies (27), to be sure that there was a significant nuclear (active) TAZ pool in human aRMS cells, we took a complementary biochemical approach and fractionated aRMS cells into cytoplasmic, nuclear, and membrane-bound compartments

(Fig. 2A). As expected (20), TAZ was predominantly cytoplasmic or membrane-bound in undifferentiated C2C12 myoblasts. On the other hand, TAZ was predominantly nuclear in both aRMS cell lines, corroborating our TMA IHC studies. We thus tested the effect of TAZ loss-of-function using RNAi, generating five independently-targeting, lentiviral-delivered, constitutive shRNAs to TAZ. Of these, two (sh2 and sh5) were selected for further study since they consistently demonstrated TAZ knockdown. Rh28 and Rh30 cells were studied in tandem, and in response to TAZ-directed shRNAs both showed *WWTR1*/TAZ suppression at the mRNA and protein levels (Fig. 2B,C). Decreased expression of TAZ target genes *CTGF* and *CYR61* verified functional knockdown (Fig. 2D,E). We next analyzed the phenotypic response to TAZ inhibition, and in cell counting assays found that, compared to the NT vector, the population growth of both cell lines declined over time (Fig. 2F,G).

TAZ suppression decreases cell proliferation, induces apoptosis, and supports myogenic differentiation in P3F-aRMS

To determine the mechanism through which TAZ suppression reduced aRMS cell growth, we examined effects on proliferation, apoptosis, and differentiation. As assessed by BrdU incorporation, TAZ suppression inhibited proliferation in both Rh28 and Rh30 cells (Fig. 2H,J). As assessed by immunoblot for cleaved PARP, TAZ suppression also induced apoptosis (Fig. 3L,M), explaining our prior observation of an increased number of floating cells during the culture of P3F-aRMS cells undergoing TAZ suppression. Last, as assessed by morphologic changes seen under light microscopy, immunocytochemistry and immunoblot for MF20 (sarcomeric myosin), and qRT-PCR for expression of *MYOD1*, *MYOG*, and *MYF6*, TAZ suppression also increased myogenic differentiation (Fig. 3A-F). Of note, increased myogenic differentiation was observed only in aRMS cells cultured in fusion media; aRMS cells cultured in normal growth media did not undergo morphologic elongation and had no or minimal increase in myogenic markers (Supplementary Fig. 4A,B). These findings were in contrast to earlier reports in C2C12 myoblasts and skeletal muscle, which showed that TAZ has a pro-differentiation effect (20,27). Given these contrasting findings, we also knocked down TAZ in C2C12 myoblasts and found that, as others had observed (20,50,51), differentiation of C2C12s is TAZ-dependent (Supplementary Fig. 4C-E). To begin to understand the differential response to TAZ suppression in transformed (aRMS) versus non-transformed (C2C12) cells, we hypothesized that the cellular response to TAZ expression might depend upon whether a cell is “poised” for differentiation, and that in a heterogeneous population we might see both phenotypes. To investigate this, we turned to a complementary gain-of-function approach and ectopically expressed a constitutively active TAZ mutant (TAZS89A, Supplementary Fig. 4F) in Rh28 and Rh30 cells. While a small proportion of the cells initially underwent a morphologic elongation reminiscent of myotubes, the majority had higher proliferation, as shown by increased BrdU incorporation (Fig. 2I,K), suggesting a heterogeneous response to TAZ expression that is cell-context dependent. In summary, TAZ suppression decreases cell proliferation, induces apoptosis, and supports myogenic differentiation in P3F-aRMS cells.

TAZ-deficient aRMS cells are enriched in the G2/M phase of the cell cycle

To determine additional mechanisms by which TAZ suppression blocks aRMS cell growth, we performed cell cycle analysis of aRMS cells stably expressing TAZ shRNAs. Compared

to the NT control vector, TAZ-deficient cells were enriched in the G2/M phase of the cell cycle (Fig. 3G,H), with an increase from 19% to 32–34% in Rh28 cells and an increase from 16% to 21–22% in Rh30 cells. To determine whether cells were arrested in G2 or M, we blotted for phospho-histone H3 (p-HH3), which is specifically phosphorylated during mitosis. We did not see an increase in p-HH3 expression with TAZ suppression in Rh28 cells (Supplementary Fig. 4G) but did see a modest increase in p-HH3 in Rh30 cells (Fig. 3I). These data suggest that TAZ depletion results in an accumulation of cells in G2/M, however a primary reduction of cells in G1/S is not ruled out and needs further study.

P3F-aRMS cancer cell stemness is TAZ-dependent

Since TAZ confers stem-like properties and chemoresistance in cancer cells of epithelial origin (21,23,24), we hypothesized that TAZ might also be important for stemness in RMS. In addition, although fusion-positive aRMS is typically sensitive to initial chemotherapy, acquired resistance and/or recurrence are common, occurring in up to 50% of cases (3). This implies that within a population of aRMS cells, some may be initially quiescent but have the ability to self-renew. To determine whether TAZ mediates P3F-aRMS stemness, we developed a 3-dimensional (3D) sphere culture system that is a well-established method for studying cancer stem cell biology (23,24), including in eRMS cells (42). We adapted an existing eRMS sphere culture protocol to permit growth of aRMS and showed that aRMS cells are also capable of forming and being propagated as spheres (Fig. 4A,C). Passaging of these aRMS spheres resulted in a 3–12 fold increase in *WWTR1* expression as measured by qRT-PCR (Fig. 4B,D), suggesting that TAZ may be important for stem cell enrichment.

We then examined whether the expression of stem cell markers *SOX2*, *OCT4*, and *NANOG* were TAZ-dependent in aRMS cells. As demonstrated via qRT-PCR, TAZ suppression led to decreased expression of these markers (Fig. 4E-H). To determine the functional role of TAZ in aRMS cancer cell stemness, we performed limiting dilution assays (LDAs) using aRMS rhabdospheres (Fig. 4I,J). We stably expressed the TAZ shRNAs or NT control in Rh28 and Rh30 cells, then plated them at varying densities. While the estimated sphere-forming frequency of the NT control for Rh28 and Rh30 cells was 1/24 and 1/21, respectively, it was reduced to <1/44 in both TAZ shRNA groups, in both cell lines. These data suggest that TAZ is functionally required for P3F-aRMS stemness and cancer cell self-renewal.

TAZ suppression attenuates tumor growth *in vivo* in Rh28 aRMS xenografts

After determining that suppression of TAZ decreases proliferation, induces apoptosis, and supports myogenic differentiation and stemness in P3F-aRMS cells *in vitro*, we used Rh28 cell xenografts to examine the role of TAZ in aRMS sarcomagenesis *in vivo*. Since constitutive suppression of TAZ in Rh28 cells inhibited cell viability, we used a conditional doxycycline (Dox)-inducible shRNA system to suppress TAZ expression after tumor formation. After validating the constructs *in vitro* (Supplementary Fig.5-6), we generated SQ xenografts and found that inducible TAZ knockdown decreased tumor growth and prolonged survival (Fig. 5A,B). By day 21, IACUC-defined maximum tumor burden was reached in all of the mice in the control groups, compared to only one tumor in the Dox groups, which had a mean day 21 tumor volume of 801mm^3. Using qRT-PCR (Fig. 5C, left) and IHC (Fig. 5D, 2nd column), we validated that TAZ suppression, including decreased nuclear TAZ

expression, (Fig. 5E, left) was maintained throughout the duration of the study at the mRNA and protein levels. We then evaluated potential mechanisms through which TAZ inhibition caused *in vivo* growth delay. We performed IHC analysis of Ki67 and TUNEL (Fig. 5D, 3rd and 4th columns) to evaluate proliferation and apoptosis, respectively. Similar to our findings *in vitro*, TAZ suppression *in vivo* led to decreased proliferation, as well as a slight increase in apoptosis (Fig. 5F,G).

While we observed tumor growth inhibition with TAZ suppression, by day 21 the mice receiving Dox began to exhibit similar growth as the control groups, suggesting the P3F-aRMS cells either developed resistance to TAZ suppression or mechanisms to compensate for TAZ inhibition. Anticipating that YAP upregulation could be a compensatory mechanism, we examined *YAP1* expression via qRT-PCR (Supplementary Fig. 7A), as well as TAZ/YAP-TEAD targets *CTGF* and *CYR61* (Fig. 5C). While *YAP1*, *CTGF*, and *CYR61* mRNA expression was slightly higher in the two Dox-treated tumors that had grown most rapidly, *YAP1* expression did not change and targets *CTGF* and *CYR61* were overall suppressed, indicating these were not mechanisms of overcoming TAZ inhibition. This result is similar to the *in vitro* observations made with TAZ suppression in C2C12 myoblasts and RD eRMS cells, where no compensatory increase in YAP expression was seen (27), and suggests that the P3F-aRMS xenografts developed alternate means for overcoming TAZ suppression.

Pharmacologic inhibition of TAZ-TEAD activity diminishes aRMS cell and tumor growth

Since TAZ is a transcriptional co-activator, it does not directly bind DNA but exerts tumorigenic activities through binding to and activating a host of oncogenic transcription factors, including TEADs (14). TEAD activity was shown to be TAZ-dependent in skeletal muscle and RD eRMS cells (27). To verify this was the case for P3F-aRMS, we transiently transfected constitutively active TAZS89A along with an 8xGTIIC TEAD reporter in Rh28 and Rh30 cells and observed a 7 to 11-fold increase in TEAD activity (Fig. 6A, Supplementary Fig. 7B).

Porphyrin compounds were identified in a drug screen to disrupt the association between YAP and TEADs (52). Although not used clinically as an anti-cancer therapy, verteporfin (VP) is FDA approved for the treatment of macular degeneration. Both VP and protoporphyrin IX (PPIX), another porphyrin derivative, are commonly used in preclinical studies of the Hippo pathway (28,52,53). We tested these compounds in the TEAD reporter assay in P3F-aRMS cells, and both drugs decreased TEAD activity (Fig. 6B,C, and Supplementary Fig. 7C-F). Additionally, VP treatment partially abrogated constitutive TAZS89A activity (Fig. 6A, Supplementary Fig.7B), and enhanced the effects of TAZ shRNA suppression (Fig. 6B). These studies suggest TEADs are activated by TAZ in P3F-aRMS, but targeting both TAZ and YAP may be necessary to completely abolish TEAD activity.

After validating target inhibition using porphyrin compounds in aRMS cells, we evaluated Rh28 cell viability following treatment with PPIX and VP. We determined that 10μM of either drug inhibits cell growth (Fig. 6D,E), which is consistent with the doses used in other cancer studies (28,52,53). We then tested these drugs on P3F-aRMS cell and tumor viability.

PPIX treatment dramatically reduced Rh28 cell growth *in vitro* as measured by cell counting over five days (Fig. 6F). Delayed tumor growth was also seen with VP treatment of Rh28 SQ xenografts *in vivo* (Fig. 6G). As tumors became palpable, mice were randomly assigned to treatment with VP or DMSO vehicle via IP injection every other day for eight doses. Similar to what was seen with VP treatment in eRMS (28), responses were variable. While a near-complete response was seen in two of the mice, one tumor grew to maximal tumor burden within the treatment observation period (Supplementary Fig. 7G,H). Although VP decreased TEAD-reporter activity *in vitro*, we did not see suppression of TEAD target genes *CTGF* and *CYR61* when examining mRNA from tumors harvested after VP treatment (Supplementary Fig. 7I), which is consistent with other observations of *in vivo* VP treatment, including in eRMS xenografts (28). Our studies suggest that targeting TAZ/YAP/TEAD pathways may be an effective treatment strategy in P3F-aRMS. However, as was observed in the TAZ shRNA xenograft studies, aRMS tumors may be able to overcome inhibition of TEAD activity, reinforcing a need for rational combination therapies.

Because TAZ suppression leads to a G2/M arrest in P3F-aRMS cells, and TAZ mediates resistance to antitubulin drugs in other malignancies (23,53–56) *in vitro*, we hypothesized that TAZ might confer resistance to VCR (the anti-microtubule agent in VAC) (3). In an MTT assay, we treated Rh28 and Rh30 cells expressing either constitutively active TAZS89A or control with varying doses of VCR and found that TAZS89A shifts the IC50 from 2.2 to 4.7 (Fig. 6H, Supplementary Fig. 7J), suggesting that TAZ promotes VCR chemoresistance in P3F-aRMS *in vitro*. We then assessed whether VP might cooperate with VCR to increase its therapeutic effect. As measured via MTT assay, an additive effect is seen in Rh28 cells treated with the combination of VCR and either 0.3μM or 1μM VP (Fig. 6I). To test whether TAZ inhibition could potentiate the effects of VCR *in vivo*, we evaluated the combination of VP and VCR in Rh28 SQ xenografts. VP was again administered every other day for eight doses and VCR was injected weekly for four doses. While efficacy was seen in monotherapy of both drugs, the combination of VP plus VCR was most effective (Fig. 6J), suggesting that TAZ-TEAD inhibition augments the activity of anti-tubulin drugs in fusion-positive aRMS.

Discussion

Although more than 20 years have passed since the PAX3-FOXO1 (P3F) fusion was discovered as the principal mutation responsible for otherwise karyotypically simple aRMS tumors, survival rates for P3F-aRMS patients remain dismal. VAC was first discovered to have activity against RMS in the 1970s, but no subsequent clinical trials have identified a more effective treatment regimen. Today, most children with P3F-aRMS will become chemo-refractory or relapse, underscoring an urgent need for novel agents that target resistance mechanisms and cancer stem cell renewal. In adult epithelial cancers, TAZ promotes metastasis, cancer stem cell-like properties, and chemoresistance [reviewed in (57–59)]. By interrogating the role of TAZ in P3F-aRMS through *in vitro* and *in vivo* genetic and pharmacologic approaches, we discovered that TAZ also mediates many of these tumorigenic traits in this mesenchymal cancer.

We have found that TAZ is highly expressed in human aRMS cells and tissue samples, with a significant fraction in the nucleus. We also found that *WWTR1* mRNA and nuclear TAZ expression are higher in aRMS tumors compared to skeletal muscle, mirroring a smaller study reporting high levels of nuclear TAZ in 6 out of 10 aRMS samples (49). Interestingly, a third analysis (using the same anti-TAZ antibody) showed TAZ staining in aRMS to be negative or cytoplasmic in the majority of tumors evaluated (27). We do not know the reason for these differences, but posit that technical differences in antigen retrieval or primary antibody incubation conditions could be responsible. Mechanistically, we find that TAZ depletion decreases aRMS cell viability and proliferation, and induces myogenic differentiation *in vitro*. TAZ is also pro-tumorigenic *in vivo*, since in murine xenograft assays TAZ suppression decreased tumor growth and proliferation, increased apoptosis, and prolonged survival. Our finding that TAZ opposes myogenic differentiation was not unexpected – indeed a signature phenotype of RMS is its loss of the ability to differentiate (60). However, since in normal skeletal myogenesis TAZ associates with MyoD and promotes differentiation, we speculate that TAZ behaves differently depending upon whether the cellular milieu (epigenetic state) is permissive for differentiation signals. This has been noted with other proteins such as mTOR, which antagonize myogenic differentiation during conditions favoring proliferation but facilitate myogenic differentiation if activated during conditions favoring differentiation (61).

Regarding the molecular relationship between TAZ and PAX3-FOXO1, it does not appear that TAZ (or for that matter YAP) are direct downstream targets of PAX3-FOXO1. As noted in our prior work, while the PAX3-FOXO1-RASSF4 axis restrains Hippo/MST1 kinase activity and *YAP1* is upregulated, RASSF-suppressed phenotypes cannot be rescued with constitutively active YAP (8). Neither do we understand why *WWTR*1/TAZ, but not *YAP1*, was uregulated in our transcriptome analysis of P3F-initiated transformation of HSMMs. However, based on studies in melanocytes, where TAZ is essential to the transcriptional activity of wild type PAX3 (29), and the fact that binding of TAZ to PAX3 occurs via domains that are retained in the P3F fusion, we hypothesize that TAZ might be a required transcriptional co-activator of P3F, and proteomic studies examining the relationship between TAZ and P3F are ongoing.

The most important translational finding from this work is that TAZ mediates aRMS cancer cell phenotypes, including supporting stemness and promoting resistance to VCR. Using novel culture conditions, we show that the functional ability of P3F-aRMS cells to form spheres is TAZ-dependent, suggesting that TAZ is critical for aRMS cell self-renewal. Although we do not know the mechanism, studies in C2C12 myoblasts show that ectopic expression of TAZS89A causes the upregulation of *Myf5* (27), a cancer stem cell gene in a zebrafish model of eRMS (62). Since most patients with aRMS who relapse are insensitive to VCR, and since TAZ mediates resistance to anti-tubulin drugs in other malignancies (23,54–56), we evaluated whether TAZ-TEAD signaling could modulate sensitivity to VCR. We found that TAZS89A decreased, while VP increased, the sensitivity of aRMS cells to VCR.

While no direct TAZ inhibitors are commercially available, TAZ is an attractive drug target due to its role in promoting stem-like properties and chemoresistance in several common

adult carcinomas. Thus, academic and pharmaceutical groups are actively investigating ways to target TAZ and/or the TAZ-TEAD interaction (58,59,63,64). While problems with solubility, toxicity and off-target effects limit their utility in patients, the efficacy of porphyrin compounds in preclinical cancer studies provides proof-of-principle that interfering with TAZ-TEAD and YAP-TEAD interactions is a promising approach. We predict that dual inhibition of TAZ and YAP may be more efficacious than monotherapy, since there is feedback between these paralogs, and inhibition of one may induce the upregulation of the other. For example, combining TAZ suppression with 5-fluorouracil paradoxically increased hepatocellular carcinoma cell growth through upregulation of YAP protein (65). In the current work, the xenograft tumors eventually grew despite TAZ RNAi or VP treatment, reinforcing the need to target TAZ in the context of rational combination therapies. On the other hand, VP combined with VCR was effective at abrogating tumor growth.

While the P3F transcription factor is currently not therapeutically tractable, inhibiting TAZ may be a means of attenuating its activity. In melanocytes, TAZ is essential to the transcriptional activity of wild type PAX3 (29,30), and the binding of TAZ to PAX3 occurs through domains that are retained in the P3F fusion (5). TEAD1 and AP-1, pro-growth transcription factors that depend on TAZ/YAP activation (10), are among the top enriched motifs in P3F binding sites (47), suggesting that these proteins may work together to control P3F-mediated transcription, a future research direction in our laboratory.

Finally, our study of TAZ biology in P3F-aRMS may shed light on the role of TAZ in sarcomas in general. A recent immunohistochemical analysis of TAZ in a range of sarcomas showed that TAZ may be associated with more undifferentiated and/or higher grade tumors (49). For example, 87% (13/15) of high-grade dedifferentiated and pleomorphic liposarcomas stained positive for nuclear TAZ, while only 6% (1/17) of low-grade myxoid and well-differentiated liposarcomas were positive. When analyzing all sarcomas, nuclear YAP and TAZ were expressed in 50% and 66% of 159 samples, respectively, and higher YAP or TAZ expression independently correlated with higher tumor grade and worse survival (49).

In conclusion, understanding TAZ biology may provide insight into molecular mechanisms of sarcomagenesis and treatment resistance (49). Here, we show that TAZ is abundant in human aRMS tumor samples, and that TAZ suppression decreases proliferation, promotes differentiation, and supports cancer cell stemness. TAZ-deficient aRMS cells are also enriched in G2/M, suggesting that TAZ may be important for G2/M cell cycle progression. Constitutive activation of TAZ diminishes the efficacy of VCR, and combining VP with VCR is more effective than either agent alone in blocking aRMS xenograft tumor growth. Inhibiting TAZ is a promising adjunctive therapy for targeting the aRMS cancer stem cell population and reducing chemoresistance.

Supplementary Material

Refer to Web version on PubMed Central for supplementary material.

Acknowledgements

We thank Drs. Dan Wechsler, David Kirsch, Gerard Blobe, Oren Becher (Duke University School of Medicine) and Erin Rudzinski (Seattle Children's) for helpful discussions and experimental suggestions. We also thank Drs. Yi-Tzu Lin, Julie Kephart, and Waitman Aumann, as well as Stefan Riedel, Margaret DeMonia, and Elaine Justice (Duke University) for technical support. The Duke Microarray and Flow Cytometry cores (Duke National Cancer Institute and a Duke Genomic and Computational Biology shared resources) provided microarray and cell cycle analyses, respectively.

Financial support

This research was supported by NIH K12 HD043494, a St. Baldrick's Foundation Fellowship, a Derfner-Children's Miracle Network Award, and the Norman & Bettina Roberts Foundation (to M.D.D.), a St. Baldrick's Summer Fellowship (to K.C.G.), NIH R01 CA122706, Alex's Lemonade Stand Innovation Award (to C.M.L.), and a Hyundai Hope on Wheels Pediatric Cancer Research Grant (to C.M.L., A.R.H.).

References

1. Hettmer S , Wagers AJ . Muscling in: Uncovering the origins of rhabdomyosarcoma. Nat Med 2010;16(2):171–3.20134473
2. Saab R , Spunt SL , Skapek SX . Myogenesis and rhabdomyosarcoma the Jekyll and Hyde of skeletal muscle. Current topics in developmental biology 2011;94:197–234.21295688
3. Arndt CA , Stoner JA , Hawkins DS , Rodeberg DA , Hayes-Jordan AA , Paidas CN , et al. Vincristine, actinomycin, and cyclophosphamide compared with vincristine, actinomycin, and cyclophosphamide alternating with vincristine, topotecan, and cyclophosphamide for intermediate-risk rhabdomyosarcoma: children's oncology group study D9803. J Clin Oncol 2009;27(31):5182–8.19770373
4. Ognjanovic S , Linabery AM , Charbonneau B , Ross JA . Trends in childhood rhabdomyosarcoma incidence and survival in the United States, 1975–2005. Cancer 2009;115(18):4218–26.19536876
5. Barr FG . Gene fusions involving PAX and FOX family members in alveolar rhabdomyosarcoma. Oncogene 2001;20(40):5736–46.11607823
6. Galili N , Davis RJ , Fredericks WJ , Mukhopadhyay S , Rauscher FJ , Emanuel BS , et al. Fusion of a fork head domain gene to PAX3 in the solid tumour alveolar rhabdomyosarcoma. Nat Genet 1993;5(3):230–5.8275086
7. Missiaglia E , Williamson D , Chisholm J , Wirapati P , Pierron G , Petel F , et al. PAX3/FOXO1 fusion gene status is the key prognostic molecular marker in rhabdomyosarcoma and significantly improves current risk stratification. J Clin Oncol 2012;30(14):1670–7.22454413
8. Crose LE , Galindo KA , Kephart JG , Chen C , Fitamant J , Bardeesy N , et al. Alveolar rhabdomyosarcoma-associated PAX3-FOXO1 promotes tumorigenesis via Hippo pathway suppression. The Journal of clinical investigation 2014;124(1):285–96.24334454
9. Pan D The hippo signaling pathway in development and cancer. Developmental cell 2010;19(4): 491–505.20951342
10. Zanconato F , Forcato M , Battilana G , Azzolin L , Quaranta E , Bodega B , et al. Genome-wide association between YAP/TAZ/TEAD and AP-1 at enhancers drives oncogenic growth. Nat Cell Biol 2015;17(9):1218–27.26258633
11. Dong J , Feldmann G , Huang J , Wu S , Zhang N , Comerford SA , et al. Elucidation of a universal size-control mechanism in Drosophila and mammals. Cell 2007;130(6):1120–33.17889654
12. Yu FX , Guan KL . The Hippo pathway: regulators and regulations. Genes Dev 2013;27(4):355–71.23431053
13. Yin MX , Zhang L . Hippo signaling: A hub of growth control, tumor suppression and pluripotency maintenance. Journal of Genetics and Genomics 2011;38(10):471–81.22035868
14. Chan SW , Lim CJ , Loo LS , Chong YF , Huang C , Hong W . TEADs mediate nuclear retention of TAZ to promote oncogenic transformation. J Biol Chem 2009;284(21):14347–58.19324876
15. Zhang H , Liu CY , Zha ZY , Zhao B , Yao J , Zhao SM , et al. TEAD Transcription Factors Mediate the Function of TAZ in Cell Growth and Epithelial-Mesenchymal Transition. Journal of Biological Chemistry 2009;284(20):13355–62.19324877

16. Bao Y , Hata Y , Ikeda M , Withanage K . Mammalian Hippo pathway: from development to cancer and beyond. J Biochem 2011;149(4):361–79.21324984
17. Morin-Kensicki EM , Boone BN , Howell M , Stonebraker JR , Teed J , Alb JG , et al. Defects in yolk sac vasculogenesis, chorioallantoic fusion, and embryonic axis elongation in mice with targeted disruption of Yap65. Mol Cell Biol 2006;26(1):77–87.16354681
18. Hossain Z , Ali SM , Ko HL , Xu J , Ng CP , Guo K , et al. Glomerulocystic kidney disease in mice with a targeted inactivation of Wwtr1. Proc Natl Acad Sci U S A 2007;104(5):1631–6.17251353
19. Judson RN , Tremblay AM , Knopp P , White RB , Urcia R , De Bari C , et al. The Hippo pathway member Yap plays a key role in influencing fate decisions in muscle satellite cells. J Cell Sci 2012;125(Pt 24):6009–19.23038772
20. Jeong H , Bae S , An SY , Byun MR , Hwang JH , Yaffe MB , et al. TAZ as a novel enhancer of MyoD-mediated myogenic differentiation. Faseb Journal 2010;24(9):3310–20.20466877
21. Chan SW , Lim CJ , Guo K , Ng CP , Lee I , Hunziker W , et al. A role for TAZ in migration, invasion, and tumorigenesis of breast cancer cells. Cancer Res 2008;68(8):2592–8.18413727
22. Li YW , Shen H , Frangou C , Yang N , Guo J , Xu B , et al. Characterization of TAZ domains important for the induction of breast cancer stem cell properties and tumorigenesis. Cell cycle (Georgetown, Tex) 2015;14(1):146–56.
23. Cordenonsi M , Zanconato F , Azzolin L , Forcato M , Rosato A , Frasson C , et al. The Hippo transducer TAZ confers cancer stem cell-related traits on breast cancer cells. Cell 2011;147(4): 759–72.22078877
24. Bhat KP , Salazar KL , Balasubramaniyan V , Wani K , Heathcock L , Hollingsworth F , et al. The transcriptional coactivator TAZ regulates mesenchymal differentiation in malignant glioma. Genes Dev 2011;25(24):2594–609.22190458
25. Xiao H , Jiang N , Zhou B , Liu Q , Du C . TAZ regulates cell proliferation and epithelial-mesenchymal transition of human hepatocellular carcinoma. Cancer science 2015;106(2):151–9.25495189
26. Tremblay AM , Missiaglia E , Galli GG , Hettmer S , Urcia R , Carrara M , et al. The Hippo transducer YAP1 transforms activated satellite cells and is a potent effector of embryonal rhabdomyosarcoma formation. Cancer Cell 2014;26(2):273–87.25087979
27. Mohamed A , Sun C , De Mello V , Selfe J , Missiaglia E , Shipley J , et al. The Hippo effector TAZ (WWTR1) transforms myoblasts and its abundance is associated with reduced survival in embryonal rhabdomyosarcoma. The Journal of pathology 2016.
28. Slemmons KK , Crose LE , Rudzinski E , Bentley RC , Linardic CM . Role of the YAP Oncoprotein in Priming Ras-Driven Rhabdomyosarcoma. PloS one 2015;10(10):e0140781.26496700
29. Murakami M , Tominaga J , Makita R , Uchijima Y , Kurihara Y , Nakagawa O , et al. Transcriptional activity of Pax3 is co-activated by TAZ. Biochem Bioph Res Co 2006;339(2):533–9.
30. Manderfield LJ , Engleka KA , Aghajanian H , Gupta M , Yang S , Li L , et al. Pax3 and hippo signaling coordinate melanocyte gene expression in neural crest. Cell Rep 2014;9(5):1885–95.25466249
31. Hazelton BJ , Houghton JA , Parham DM , Douglass EC , Torrance PM , Holt H , et al. Characterization of cell lines derived from xenografts of childhood rhabdomyosarcoma. Cancer Res 1987;47(16):4501–7.3607778
32. Douglass EC , Valentine M , Etcubanas E , Parham D , Webber BL , Houghton PJ , et al. A specific chromosomal abnormality in rhabdomyosarcoma. Cytogenet Cell Genet 1987;45(3–4):148–55.3691179
33. Khan J , Simon R , Bittner M , Chen Y , Leighton SB , Pohida T , et al. Gene expression profiling of alveolar rhabdomyosarcoma with cDNA microarrays. Cancer Res 1998;58(22):5009–13.9823299
34. Taylor AC , Shu L , Danks MK , Poquette CA , Shetty S , Thayer MJ , et al. P53 mutation and MDM2 amplification frequency in pediatric rhabdomyosarcoma tumors and cell lines. Med Pediatr Oncol 2000;35(2):96–103.10918230

35. Barr FG , Nauta LE , Davis RJ , Schafer BW , Nycum LM , Biegel JA . In vivo amplification of the PAX3-FKHR and PAX7-FKHR fusion genes in alveolar rhabdomyosarcoma. Hum Mol Genet 1996;5(1):15–21.8789435
36. Naini S , Etheridge KT , Adam SJ , Qualman SJ , Bentley RC , Counter CM , et al. Defining the cooperative genetic changes that temporally drive alveolar rhabdomyosarcoma. Cancer Res 2008;68(19047133):9583–8.19047133
37. Linardic CM , Naini S , Herndon JE , Kesserwan C , Qualman SJ , Counter CM . The PAX3-FKHR fusion gene of rhabdomyosarcoma cooperates with loss of p16INK4A to promote bypass of cellular senescence. Cancer Res 2007;67(14):6691–9.17638879
38. Zhou Z , Hao Y , Liu N , Raptis L , Tsao MS , Yang X . TAZ is a novel oncogene in non-small cell lung cancer. Oncogene 2011;30(18):2181–6.21258416
39. Zhao B , Wei X , Li W , Udan RS , Yang Q , Kim J , et al. Inactivation of YAP oncoprotein by the Hippo pathway is involved in cell contact inhibition and tissue growth control. Gene Dev 2007;21(21):2747–61.17974916
40. Belyea BC , Naini S , Bentley RC , Linardic CM . Inhibition of the Notch-Hey1 axis blocks embryonal rhabdomyosarcoma tumorigenesis. Clin Cancer Res 2011;17(23):7324–36.21948088
41. Fang Y , Linardic CM , Richardson DA , Cai W , Behforouz M , Abraham RT . Characterization of the cytotoxic activities of novel analogues of the antitumor agent, lavendamycin. Molecular cancer therapeutics 2003;2(6):517–26.12813130
42. Walter D , Satheesha S , Albrecht P , Bornhauser BC , D'Alessandro V , Oesch SM , et al. CD133 positive embryonal rhabdomyosarcoma stem-like cell population is enriched in rhabdospheres. PloS one 2011;6(5):e19506.21602936
43. Hu Y , Smyth GK . ELDA: extreme limiting dilution analysis for comparing depleted and enriched populations in stem cell and other assays. J Immunol Methods 2009;347(1–2):70–8.19567251
44. Kephart JJ , Tiller RG , Crose L , Slemmons KK , Chen PH , Hinson AR , et al. Secreted frizzled related protein 3 (SFRP3) is required for tumorigenesis of PAX3-FOXO1-positive alveolar rhabdomyosarcoma. Clin Cancer Res 2015.
45. Naini S , Etheridge KT , Adam SJ , Qualman SJ , Bentley RC , Counter CM , et al. Defining the cooperative genetic changes that temporally drive alveolar rhabdomyosarcoma. Cancer Res 2008;68(23):9583–8.19047133
46. Hosoyama T , Aslam MI , Abraham J , Prajapati SI , Nishijo K , Michalek JE , et al. IL-4R drives dedifferentiation, mitogenesis, and metastasis in rhabdomyosarcoma. Clin Cancer Res 2011;17(9): 2757–66.21536546
47. Cao L , Yu Y , Bilke S , Walker RL , Mayeenuddin LH , Azorsa DO , et al. Genome-wide identification of PAX3-FKHR binding sites in rhabdomyosarcoma reveals candidate target genes important for development and cancer. Cancer Res 2010;70(16):6497–508.20663909
48. Khan JT,T NCI OncoGenomics DB. <https://pob.abcc.ncifcrf.gov/cgi-bin/JK>.
49. Fullenkamp CA , Hall SL , Jaber OI , Pakalniskis BL , Savage EC , Savage JM , et al. TAZ and YAP are frequently activated oncoproteins in sarcomas. Oncotarget 2016.
50. Park GH , Jeong H , Jeong MG , Jang EJ , Bae MA , Lee YL , et al. Novel TAZ modulators enhance myogenic differentiation and muscle regeneration. British journal of pharmacology 2014;171(17):4051–61.24821191
51. Yang Z , Nakagawa K , Sarkar A , Maruyama J , Iwasa H , Bao Y , et al. Screening with a novel cell-based assay for TAZ activators identifies a compound that enhances myogenesis in C2C12 cells and facilitates muscle repair in a muscle injury model. Mol Cell Biol 2014;34(9):1607–21.24550007
52. Liu-Chittenden Y , Huang B , Shim JS , Chen Q , Lee S-J , Anders RA , et al. Genetic and pharmacological disruption of the TEAD-YAP complex suppresses the oncogenic activity of YAP. Gene Dev 2012;26(12):1300–5.22677547
53. Brodowska K , Al-Moujahed A , Marmalidou A , Meyer Zu Horste M , Cichy J , Miller JW , et al. The clinically used photosensitizer Verteporfin (VP) inhibits YAP-TEAD and human retinoblastoma cell growth in vitro without light activation. Experimental eye research 2014;124:67–73.24837142

54. Lai D , Ho KC , Hao Y , Yang X . Taxol resistance in breast cancer cells is mediated by the hippo pathway component TAZ and its downstream transcriptional targets Cyr61 and CTGF. Cancer Res 2011;71(7):2728–38.21349946
55. Bartucci M , Dattilo R , Moriconi C , Pagliuca A , Mottolese M , Federici G , et al. TAZ is required for metastatic activity and chemoresistance of breast cancer stem cells. Oncogene 2015;34(6):681–90.24531710
56. Zhao Y , Yang X . Regulation of sensitivity of tumor cells to antitubulin drugs by Cdk1-TAZ signalling. Oncotarget 2015;6(26):21906–17.26183396
57. Mo JS , Park HW , Guan KL . The Hippo signaling pathway in stem cell biology and cancer. Embo Reports 2014;15(6):642–56.24825474
58. Johnson R , Halder G . The two faces of Hippo: targeting the Hippo pathway for regenerative medicine and cancer treatment. Nature reviews Drug discovery 2014;13(1):63–79.24336504
59. Harvey KF , Zhang X , Thomas DM . The Hippo pathway and human cancer. Nat Rev Cancer 2013;13(4):246–57.23467301
60. Keller C , Guttridge DC . Mechanisms of impaired differentiation in rhabdomyosarcoma. The FEBS journal 2013;280(17):4323–34.23822136
61. Wilson RA , Liu J , Xu L , Annis J , Helmig S , Moore G , et al. Negative regulation of initial steps in skeletal myogenesis by mTOR and other kinases. Scientific reports 2016;6:20376.26847534
62. Ignatius MS , Chen E , Elpek NM , Fuller AZ , Tenente IM , Clagg R , et al. In vivo imaging of tumor-propagating cells, regional tumor heterogeneity, and dynamic cell movements in embryonal rhabdomyosarcoma. Cancer Cell 2012;21(5):680–93.22624717
63. Moroishi T , Hansen CG , Guan KL . The emerging roles of YAP and TAZ in cancer. Nat Rev Cancer 2015;15(2):73–9.25592648
64. Park HW , Guan KL . Regulation of the Hippo pathway and implications for anticancer drug development. Trends in pharmacological sciences 2013;34(10):581–924051213
65. Hayashi H , Higashi T , Yokoyama N , Kaida T , Sakamoto K , Fukushima Y , et al. An Imbalance in TAZ and YAP Expression in Hepatocellular Carcinoma Confers Cancer Stem Cell-like Behaviors Contributing to Disease Progression. Cancer Res 2015;75(22):4985–97.26420216

Statement of Translational Relevance

Alveolar rhabdomyosarcoma (aRMS) is a soft tissue sarcoma associated with the skeletal muscle lineage, affecting mostly children and adolescents. aRMS tumors are characterized by the *PAX3-FOXO1* fusion gene, a chimeric transcription factor thought to illegitimately reactivate embryonic myogenesis programs. While the majority of aRMS tumors initially respond to multi-modal therapy, most will become resistant, underscoring the 5-year survival rate of <50% for all-comers and <10% when metastatic. Understanding the mechanisms responsible for aRMS cell self-renewal and chemoresistance is critical. In adult carcinomas, the TAZ transcriptional co-activator (encoded by the *WWTRI* gene and a paralog of the Hippo pathway effector YAP) has been found to support tumor cell proliferation, survival, and stemness. Far less is known about the role of TAZ in sarcomas, including aRMS. Here, we show that TAZ is highly expressed in human aRMS tumors and supports aRMS tumorigenic phenotypes *in vitro* and *in vivo*. Suppression of TAZ through genetic or pharmacologic approaches diminishes aRMS tumor growth and prolongs survival in xenograft studies, and potentiates the activity of the antitubulin agent vincristine, a standard agent in aRMS therapy. These studies identify TAZ inhibition as a potential adjunct therapy to target fusion-positive aRMS stemness and chemoresistance.

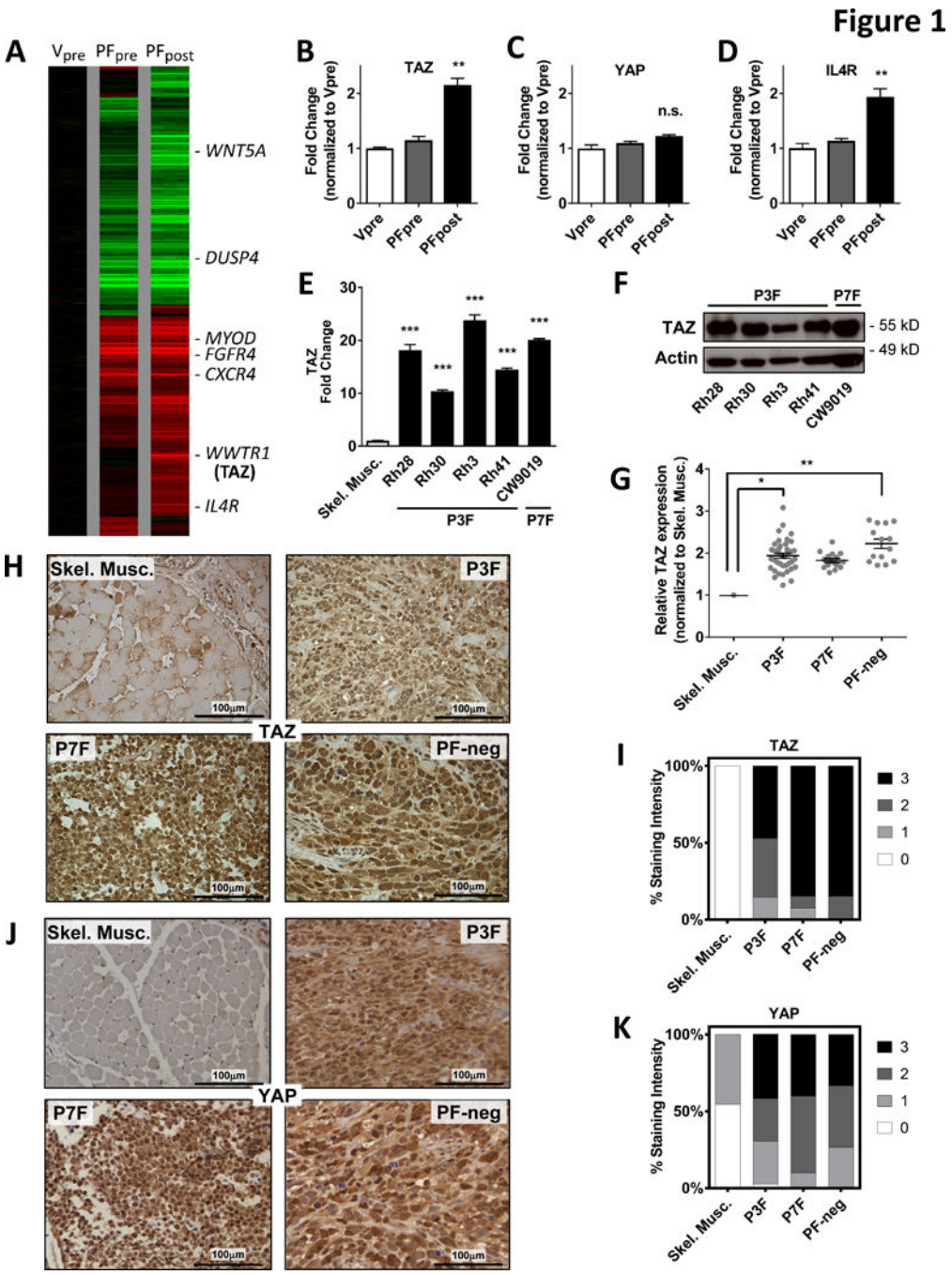

Figure 1. TAZ is upregulated in PAX3-FOXO1-expressing primary human skeletal muscle myoblasts, aRMS cell lines, and tumors.

(A) Expression profile of human skeletal muscle myoblast (HSMM) vector control cells (Vpre) compared with PAX3-FOXO1 (P3F)–expressing HSMM cells pre-senescence bypass (PFpre) or post-senescence bypass (PFpost). This image is modified with permission from the *Journal of Clinical Investigation*. Portions of these data and validation of internal controls (*WNT5A, DUSP4, MYOD, FGFR4, CXCR4*) were previously reported (8,44). qRT-PCR verifies **(B)** increased *WWTR1* (TAZ) expression, **(C)** unchanged YAP

expression, and **(D)** validation of *IL4R* as a low-expressing internal control gene induced by P3F (46,47). As measured by **(E)** qRT-PCR and **(F)** immunoblot, P3F and P7F human aRMS cell lines express high levels of TAZ compared to human skeletal muscle. **(G)** From microarray data in the Oncogenomics database (48), TAZ expression is higher in fusion-positive and fusion-negative primary human aRMS tumors than in human skeletal muscle. Representative images of RMS TMA cores immunostained for **(H)** TAZ and **(I)** YAP protein. Scale bars, 100μm. Quantification of **(J)** TAZ and **(K)** YAP staining in RMS shows increased expression of both proteins. For TAZ staining, Muscle, N=11; P3F, N=34; P7F, N=13; PF-neg, N=13. For YAP staining, Muscle, N=11; P3F, N=36; P7F, N=10; PF-neg, N=15. While the gene name for TAZ is *WWTR1*, for simplicity the label TAZ is used throughout the remainder of the figures.

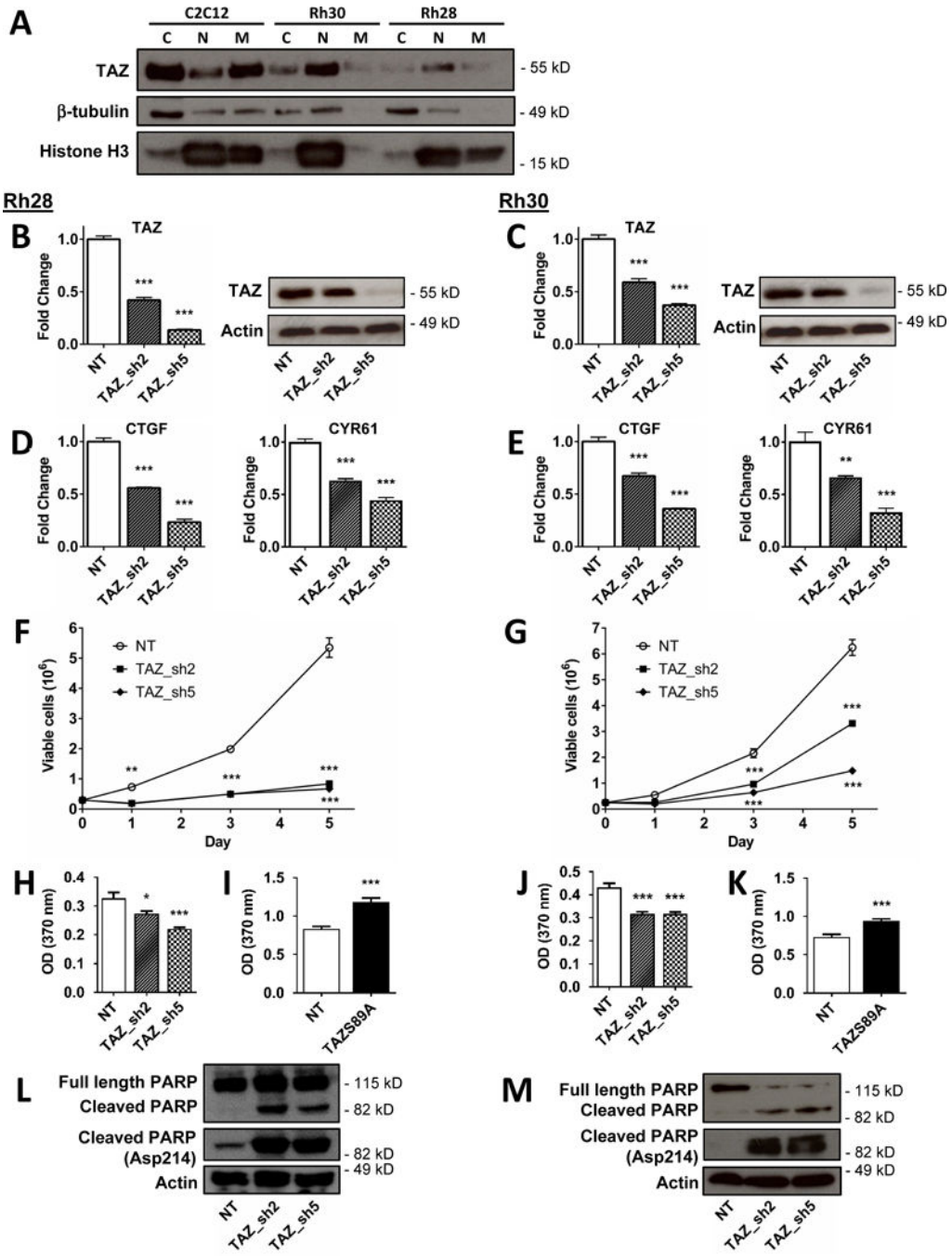

Figure 2. Genetic suppression of TAZ inhibits aRMS cell growth, decreases cell proliferation, and increases apoptosis.

(A) Cell fractionation reveals enrichment of nuclear (active) TAZ in Rh28 and Rh30 aRMS cells, compared to primarily cytoplasmic/membrane expression in C2C12 murine myoblasts. β-tubulin and histone H3 are used as markers of cytoplasmic and nuclear expression. **(B, C)** Lentiviral-mediated suppression of TAZ in Rh28 and Rh30 cells shows consistent knockdown as measured by qRT-PCR and immunoblot. TAZ knockdown also leads to **(D, E)** suppression of TAZ target genes *CTGF* and *CYR61* as measured by qRT-PCR, **(F, G)**

decreased cell growth as measured by cell counting in culture, and **(H, J)** decreased proliferation as measured by BrdU incorporation. Conversely, aRMS cells expressing constitutively active TAZ (TAZS89A) show increased proliferation **(I, K)**. TAZ suppression also led to increased apoptosis, as measured by immunoblots of both full length and cleaved PARP **(L, M)**. Actin used as loading control. C, cytoplasmic; N, nuclear; M, membrane; NT, non-targeting scrambled control vector. *, $P<0.05$; **, $P<0.01$; and ***, $P<0.001$.

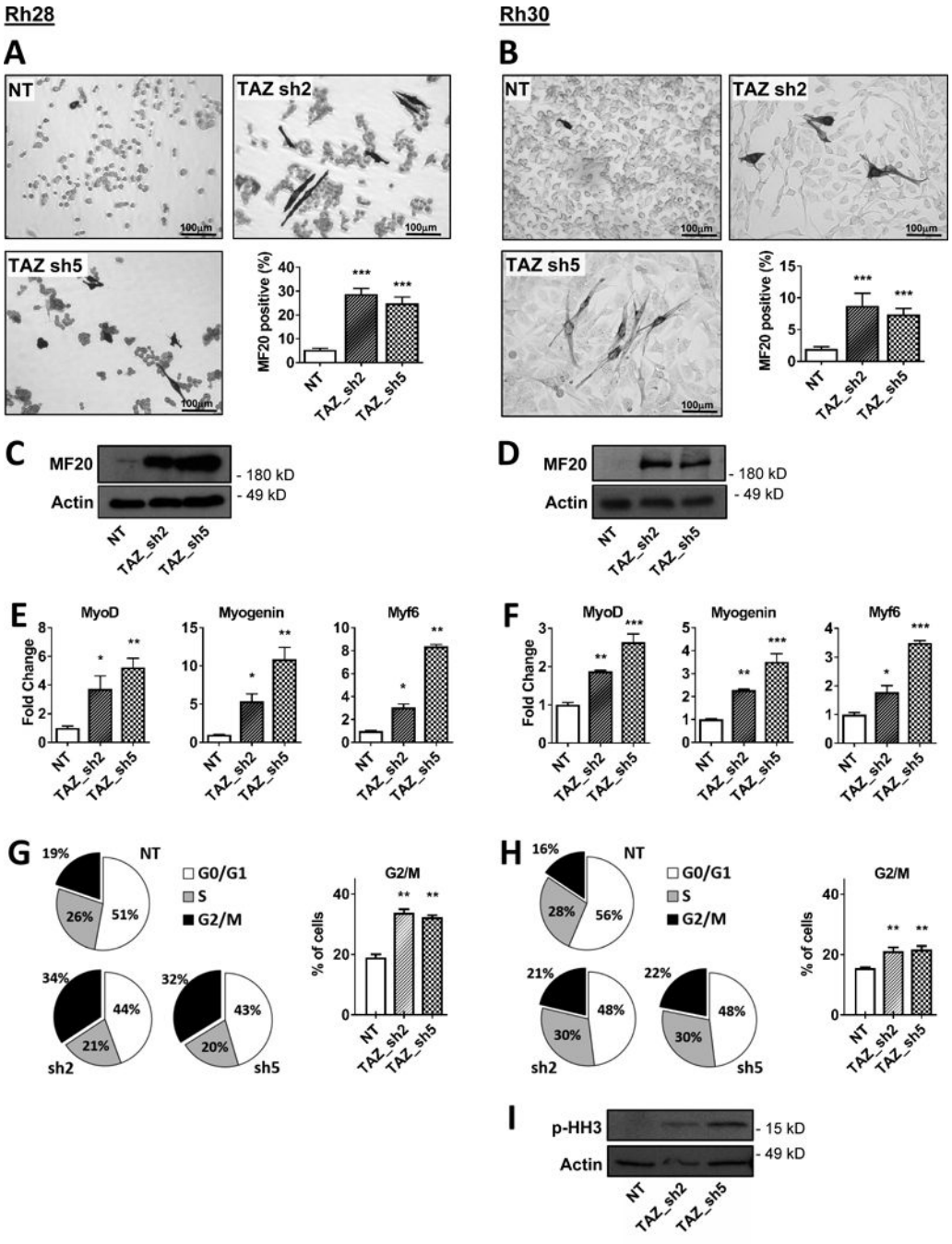

Figure 3. TAZ suppression promotes myogenic differentiation, and enriches the G2/M population.

(A, B) Rh28 and Rh30 cells stably expressing TAZ shRNAs and cultured in differentiation-inducing conditions display morphologic elongation as well as increased staining for MF20 (myosin heavy chain) expression, **(C, D)** increased MF20 expression as measured by immunoblot, and **(E, F)** increased myogenic marker expression as measured by qRT-PCR. Scale bars, 100μm. **(G, H)** Rh28 and Rh30 cells stably expressing TAZ shRNAs show an increase in the G2/M phase of the cell cycle as measured by flow cytometry of DNA

content. Bars represent the average and SE of each group. N=3 (Rh28s), N=2 (Rh30s). **(I)** As measured by immunoblot for M-phase specific phosphorylation of histone H3, TAZ suppression in Rh30 cells leads to an accumulation of cells in M phase. Actin used as loading control. NT, non-targeting scrambled control vector.

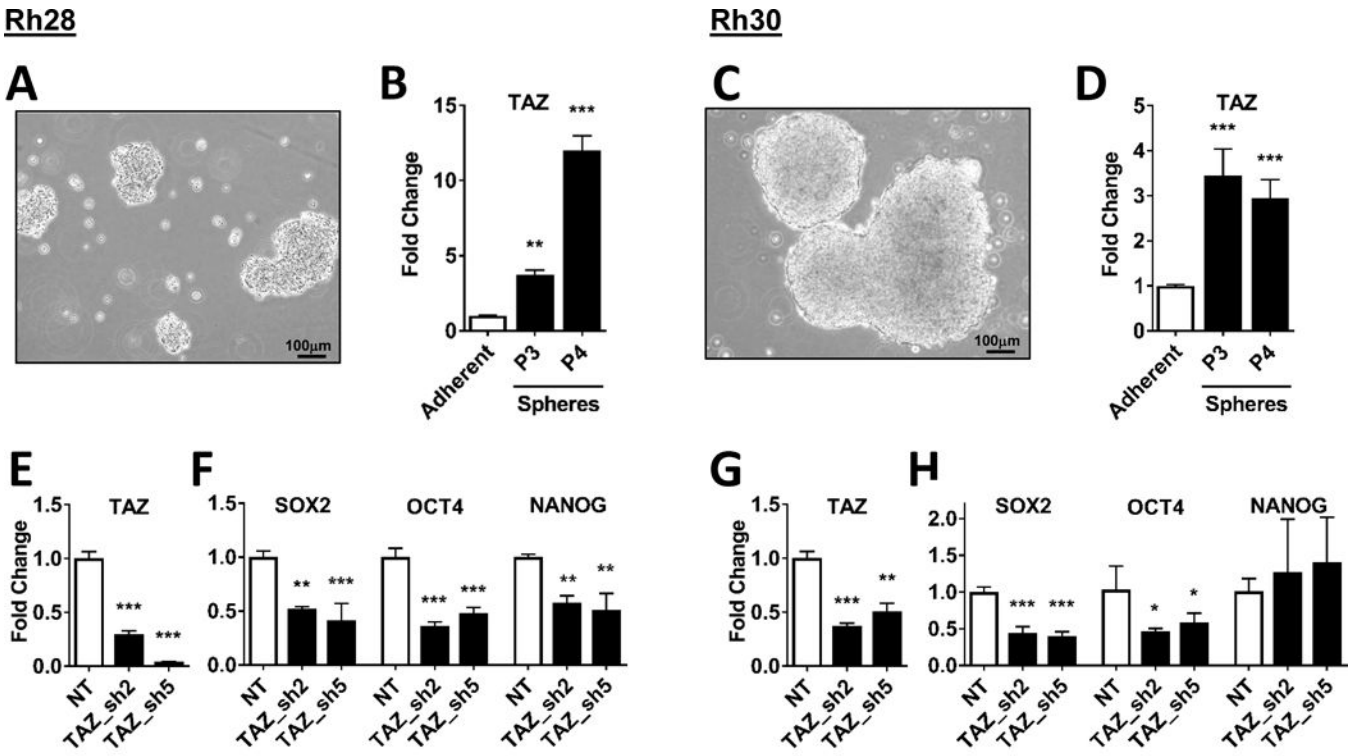

I

Rh28 rhabdosphere forming frequency

# cells per well	# wells plated	# of wells with spheres		
		NT	TAZ_sh2	TAZ_sh5
100	48	48	43	43
75	48	46	33	39
50	48	42	28	31
25	48	29	13	14
Sphere-forming frequency (95% CI)		1/24 (1/20-1/29)	1/58 (1/48-1/70)	1/49 (1/41-1/60)
P value			<0.0001	<0.0001

J

Rh30 rhabdosphere forming frequency

# cells per well	# wells plated	# of wells with spheres		
		NT	TAZ_sh2	TAZ_sh5
100	48	48	34	46
60	48	48	13	42
30	48	40	4	18
10	48	3	0	0
Sphere-forming frequency (95% CI)		1/21 (1/17-1/27)	1/142 (1/108-1/186)	1/44 (1/36-1/54)
P value			<0.0001	<0.0001

Figure 4. TAZ supports and is necessary for aRMS cancer cell stemness.

Rh28 (*left*) and Rh30 (*right*) aRMS cells were grown as 3D-rhabdospheres. **(A, C)** Representative images of spheres. Scale bars, 100μm. **(B, D)** Compared to cells grown as an adherent monolayer, serial sphere passage increases TAZ expression, as measured by qRT-PCR. TAZ suppression **(E, G)** also leads to **(F, H)** decreased expression of stem cell genes *SOX2*, *OCT4*, and *NANOG*, as measured by qRT-PCR. mRNA expression was normalized to GAPDH. **(I, J)** Limiting dilution assays in cells stably expressing TAZ shRNAs show TAZ is necessary for stem cell renewal in aRMS cells. The average sphere-forming frequency is shown, with the expected range in parentheses. During LDA optimization, neither Rh28 nor Rh30 cells were able to form spheres when plated at 1 cell/well, and compared to Rh30 cells, Rh28 cells were less able to form spheres at lower cell densities. P=passage number.

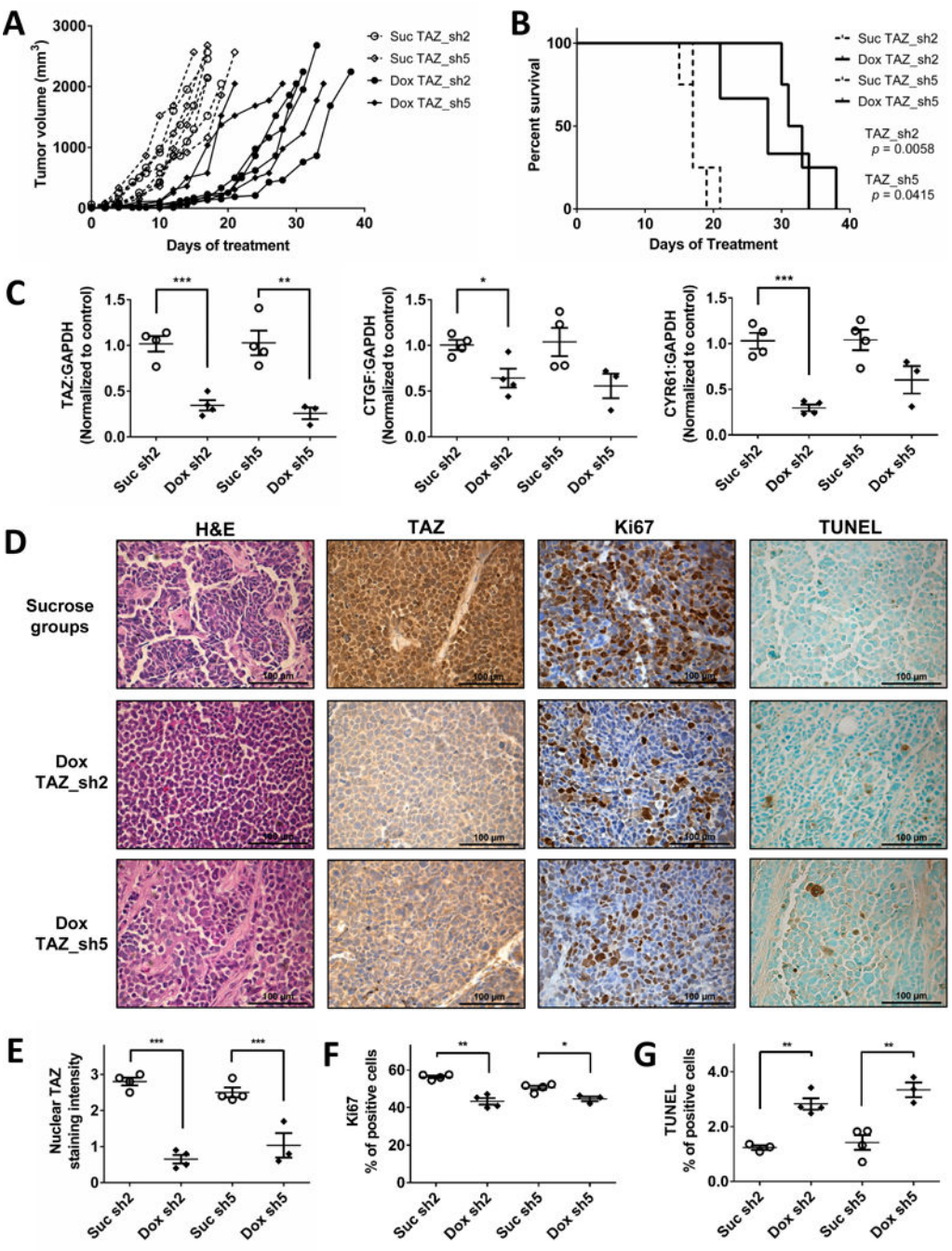

Figure 5. Suppression of TAZ inhibits aRMS tumor growth and prolongs survival in murine xenografts.

TAZ suppression in Rh28 xenografts **(A)** delays tumor progression, as measured by time to maximum tumor burden, and **(B)** prolongs survival as measured by Kaplan-Meier survival plot. Median survival and 95% confidence interval for the groups were: Suc sh2 (17.5 ± 0.98 days), Dox sh2 (33 ± 3.49 days), Suc sh5 (17.5 ± 2.47 days), and Dox sh5 (30 ± 3.39 days). **(C)** qRT-PCR validation of TAZ suppression and downregulation of TAZ target genes (*CTGF*, *CYR61*). **(D)** Representative IHC images of H&E, TAZ, Ki67, and TUNEL staining

for each of the groups. IHC quantitation showing the TAZ shRNA groups have **(E)** decreased nuclear TAZ staining, **(F)** decreased proliferation (Ki67), and **(G)** increased apoptosis (TUNEL). Scale bars: 100μm. N=4 in each arm except Dox TAZ_sh5 group, where one mouse did not develop a tumor so N=3.

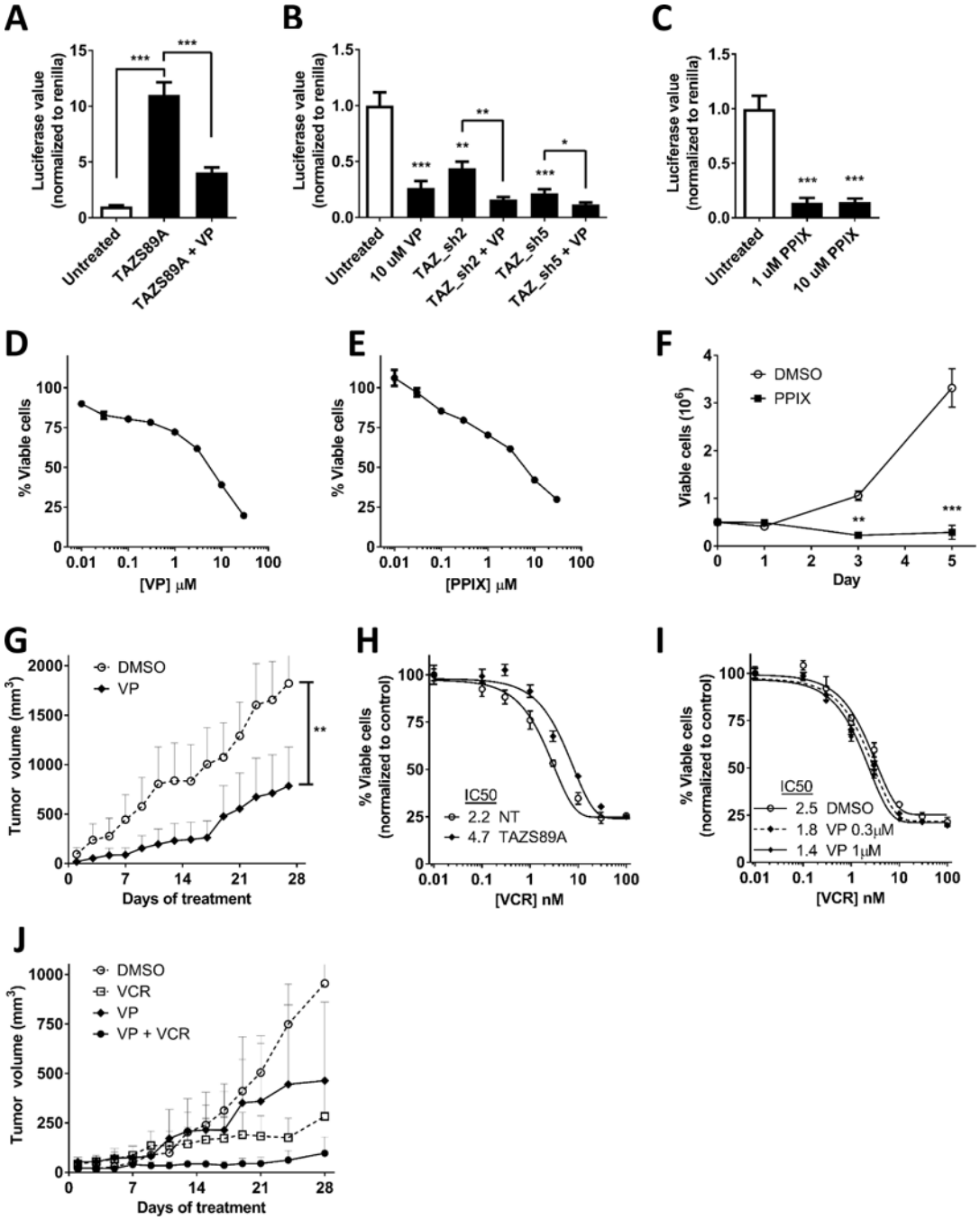

Figure 6. Pharmacologic inhibition of TAZ-TEAD activity diminishes aRMS cell and tumor growth.

TEAD luciferase activity (8XGTIIC–Luc reporter) is **(A)** increased in Rh28 cells expressing constitutively activate TAZ mutant TAZS89A, but partially reversible with treatment of 10μM VP, **(B)** decreased in Rh28 cells treated with 10μM VP, as well as in Rh28 cells stably expressing TAZ shRNAS; and **(C)** decreased in Rh28 cells treated with 1μM or 10μM PPIX. **(D, E)** Dose response curve in Rh28 cells treated with VP or PPIX. **(F)** Rh28 cells treated with 10μM PPIX have decreased cell growth, as measured by manual cell counting. **(G)**

Rh28 xenografts treated with 100mg/kg VP have decreased tumor growth as compared to vehicle control (DMSO). **(H)** TAZS89A decreases Rh28 cell sensitivity to VCR. **(I)** Dose-dependent cooperativity with either 0.3μM or 1μM VP and VCR in Rh28 cells. **(J)** The combination of VP and VCR *in vivo* is more effective than either agent alone in inhibiting tumor growth. N = 5 mice in each group. VP, verteporfin; PPIX, protoporphyrin IX.